Microfluid Nanofluid
DOI 10.1007/s10404-013-1189-6

RESEARCH PAPER

Circuit model for microfluidic bubble generation under controlled pressure

Shu-che Peng · Shailesh P. Nagarkar · Justin L. Lowen · Sachin S. Velankar

Received: 3 December 2012 / Accepted: 6 April 2013

Abstract We explore the microfluidic generation of bubbles in a flow-focusing junction using a pressure-controlled device rather than the more common flow rate-controlled devices. This device is a prototype for extending microfluidic drop generation methods to molten polymers. We show that the bubble generation process is highly sensitive to pressure: small changes in pressure induce large changes in bubble size and bubble formation frequency. A simple resistance circuit model can explain this pressure dependence. Briefly, we show that bubble generation is possible only within a finite pressure range. Near the ends of this pressure range, the ratio of the flow rates of the dispersed to continuous phase is highly sensitive to pressure, and therefore so also is the bubble generation process. The circuit model offers a way to use existing models of drop generation (which are based on flow rate-controlled operation) to predict pressure-controlled operation. We also examine drop formation using a highly viscous polymer as the dispersed phase. Drops are formed far downstream of the flow-focusing junction, and they are far smaller than the microfluidic channel dimensions. These results suggest that existing microfluidic drop generation methods may be exploited to make complex particles from thermoplastic polymers.

Keywords Drop generation · Bubbles · Particle synthesis · Molten polymer · Pressure-driven flow

1 Introduction

In a majority of microfluidics research, the flow is driven by external syringe pumps. Since these are positive displacement pumps, the flow rate is specified; in this article, we will refer to this situation as "flow rate-controlled". In a minority of situations, however, flow is driven by an applied pressure, typically maintained with a gravitational head or with pressure regulators. Such "pressure-controlled" devices are advantageous in some applications in that flow can be started or stopped rapidly, limited only by the speed of valve actuation (Bong et al. 2010). In contrast, when syringe pumps are used, there is often a long transient associated with the compliance of the tubing connecting the device to the pump (Stone et al. 2004). We are interested in microfluidics using molten polymers (Moon and Migler 2010; Moon et al. 2008), and for that purpose, pressure-controlled flow is especially convenient as will be discussed briefly below.

This article is concerned with bubble or drop generation under controlled pressure conditions. Two-phase microfluidic devices that generate drops or bubbles have been studied intensively for several years (Thorsen et al. 2001; Christopher and Anna 2007; Cubaud and Mason 2008; Sugiura et al. 2001). Most such devices operate passively, i.e., the two fluids are combined together at a junction and drops are formed spontaneously by an interfacial tension-driven pinch off process. Such passive drop-generating devices can be operated in flow rate-controlled fashion (Nie et al. 2006; Anna et al. 2003; Cubaud et al. 2005), or in pressure-controlled fashion (Thorsen et al. 2001), or in a

Electronic supplementary material The online version of this article (doi:10.1007/s10404-013-1189-6) contains supplementary material, which is available to authorized users.

S. Peng · S. P. Nagarkar · J. L. Lowen · S. S. Velankar (✉)
Department of Chemical Engineering,
University of Pittsburgh, Pittsburgh, PA 15261, USA
e-mail: velankar@pitt.edu

Published online: 21 April 2013

combination of the two (Garstecki et al. 2004). In elegant experiments, Ward et al. (2005) compared pressure-controlled versus flow rate-controlled drop generation in the same device. The controlled parameters were the ratio of flow rates of the two phases (in the flow rate-controlled experiments) and the ratio of the pressures (in the pressure-controlled experiments). The most important difference noted between the two cases was the sensitivity: in the pressure-controlled situation, the drop size and frequency were highly sensitive to the pressure ratio, whereas in the rate-controlled situation, the sensitivity was much less. The authors did not fully explain the reasons for these differences but speculated that there was a fundamental difference between drop generation in these two situations. This paper develops a simple circuit model to explain the reasons for this difference.

Before proceeding with the main results of the paper, we will briefly provide some motivation for these experiments. This article is a part of an effort to develop a new platform for two-phase drop microfluidics with molten polymers. The goal is to use microfluidic devices to fabricate complex particles from thermoplastic polymers. Drop-based microfluidics has been used previously to prepare particles with complex shapes or chemical anisotropies(Marre and Jensen 2010; Nie et al. 2006; Dendukuri et al. 2005; Chen et al. 2009; Serra and Chang 2008), and much of this research has been reviewed in an excellent book on this topic(Kumacheva and Garstecki 2011). Most of those methods rely upon using a UV-curable monomer as the drop phase: after the drop is generated, it is crosslinked rapidly by UV exposure. The requirement of rapid crosslinking by UV radiation limits this approach to a relatively narrow range of material chemistries. Other approaches of solidifying drops such as sol–gel chemistry, phase separation, or solvent extraction can access a wider range of material types including ceramics or polymers (Marre and Jensen 2010; Shum et al. 2010). However, an even greater range of material properties may be accessed using thermoplastic polymers. The overall idea then is to develop microfluidic devices that generate polymer drops at high temperature under molten conditions, and then convert them into particles by simply cooling the flow stream.

The requirements of operating at high temperature and with fluids of high viscosity raise new challenges in fluids handling. Recent research has developed devices and fluids handling methods that address these practical challenges (Moon and Migler 2010; Moon et al. 2008). Most importantly, Moon et al. fabricate microchannels using etched metal foils and use gas pressure rather than syringe pumps to drive flow. Beyond resolving these practical challenges, however, for our present goal of drop generation, there is also a fundamental difficulty: the viscosity of molten polymers is typically 4–7 orders of magnitude higher than of small molecule systems, and thus, it is not clear whether passive drop breakup—which is entirely driven by interfacial tension—can successfully pinch off drops within reasonable timescales. The experiments in this article were conducted chiefly to test the last question. Specifically, we examine bubble and drop generation when the fluids have a high viscosity typical of molten polymers. The experiments were conducted at room temperature for convenience; however, the device was designed to be readily adaptable to high temperature.

2 Experimental

Experiments were conducted at room temperature with polydimethylsiloxane (PDMS) as the continuous phase fluid. The experiments discussed here used a viscosity of 30 Pa.s; however, we have conducted similar experiments with PDMS of viscosity 10 and 500 Pa.s and obtained essentially identical results (Peng 2012). Although these viscosities are many orders of magnitude higher than encountered in aqueous systems, they are typical for molten polymers. In most of this article, the dispersed phase was nitrogen gas. In the last section, we will briefly discuss experiments with another polymer, polyisoprene (Kuraray America), as the dispersed phase. It had a viscosity of 120 Pa.s.

The microfluidic device (Fig. 1a, b) used here is based on an approach developed previously (Moon and Migler 2010; Moon et al. 2008) in which the microchannels were laser-machined out of thin brass foils. Such metal foils can be used at high temperatures with molten polymers, although this article only refers to room temperature. The foils are sandwiched between a lower acrylic plate and an upper acrylic block which also provided the fluidic connections. The entire assembly was bolted to a bottom aluminum plate with a long slot (Fig. 1b) to permit imaging with an inverted microscope. The acrylic block had two fluid reservoir chambers which could be pressurized using gas pressure regulators (Masoneilan 78–4) supplied by a nitrogen tank. The pressure was monitored downstream of the regulator using Honeywell 26PC15 pressure sensors connected to a computer. Drop generation was observed using an Olympus CKX inverted microscope with a 4× objective using an Edmund Optics EO-1312 M camera operating at 13 frames/s. At the driving pressures used, the high viscosity fluids give relatively low drop production frequencies (on the order of a few Hz) which can be resolved even without a high speed camera.

The junction of the channel had a "flow-focusing" geometry which was realized using three stacked metal foil layers. The channels machined into each layer are

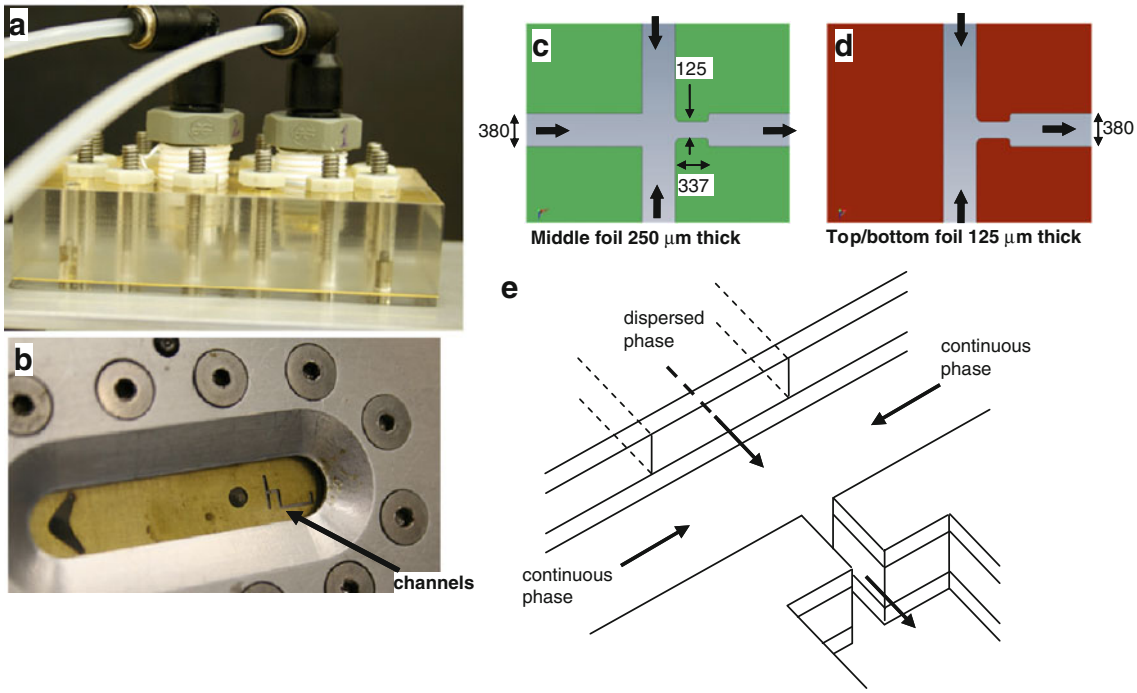

Fig. 1 **a** Picture of the microfluidic device. The metal foil is visible as a *slim yellow line* near the base of the device. **b** Inverted view of the device showing the channels. **c** Channels machined in the middle layer of metal foil. **d** Channels in the *top* and *bottom* layers of metal foils. **e** Schematic of the microfluidic flow-focusing junction. Note that the air supply channel is in the middle layer only. The numbers in **c** and **d** are channel widths in microns

illustrated in Fig. 1c, d, and upon stacking them, the flow-focusing junction of Fig. 1e was realized.[1]

A few drops of PDMS were placed in the reservoir chamber for the continuous phase, whereas the other reservoir was left empty. Upon applying pressure, the PDMS as well as the nitrogen were forced from the reservoir into the microfluidic channels. Each experiment started with a specific pressure P_c applied to the continuous phase PDMS, and the pressure P_d of the dispersed phase nitrogen was increased in a stepwise fashion. Each pressure was maintained for at least 3 min to verify that the drop generation process remained invariant. During these 3 min, the pressures varied by <0.01 psi.

3 Results

Figure 2 shows the results of a typical experiment of increasing P_d from an initially small value while keeping P_c fixed. At low values of P_d, no bubbles were generated; instead, backflow of the PDMS into the nitrogen supply channel was observed. At some value of P_c, the backflow stopped and the gas flowed into the junction forming bubbles with frequencies in the 0.5–5 Hz range (discussed later). Images of bubbles in the junction and in the downstream channel are shown in Figs. 2a, b. Upon increasing P_d, the bubble size and frequency both increased (Fig. 2c, d) until at some value of P_d, bubble pinch off no longer happened; instead, an irregular coflow of gas and PDMS was observed (Fig. 2e, f). After the onset of coflow, P_d was reduced back to a low value, and the entire procedure repeated at a different value of P_c. In a limited number of experiments, the P_d was reduced gradually, and in these cases, no hysteresis was apparent: the bubble size and frequency as P_d was reduced matched that as P_d was increased. Sample movies of the bubbles and coflow at P_c= 8 psi are provided as Online Supplementary information. Figure 2g maps the conditions of pressure under which bubbles were formed. It is immediately obvious that the process is extremely sensitive to pressure: at fixed P_c the transition from back flow to bubble generation to coflow all happened over at most 10 % changes in pressure P_d.

We will now examine the bubble size, which is usually quantified in terms of the length, L. In many cases, the bubbles had a small concave region at the back end making it somewhat difficult to identify L from the image directly.

[1] As mentioned in the Introduction, this project is motivated by our interest in drop microfluidics with molten polymers. Unlike with oil/water systems, with immiscible polymers, we are unable to find suitable surfactants that can guarantee that the walls of the device remain wetted by the continuous phase. Thus, it is crucial to ensure that the dispersed phase does not contact the walls, which is the purpose of the three-layer design.

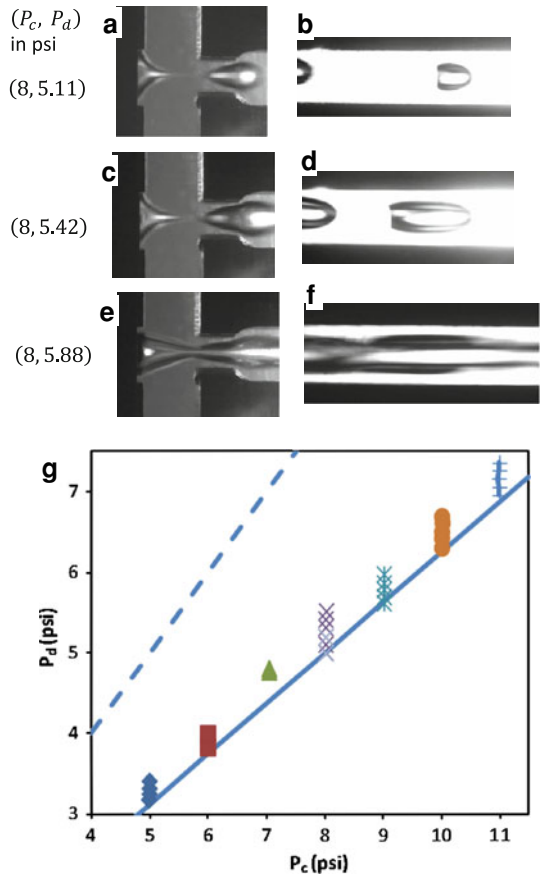

Fig. 2 **a–f** Images of bubbles at the pressure values indicated on the left of the images. The *left column* of images was taken at the junction, and the *right column* in the downstream channel. **g** The combinations of pressure at which two-phase flow was observed. *Dashed* and *solid lines* refer to Eqs. (10) and (11), respectively, in the text

Accordingly, a simple image analysis procedure was used to obtain L as described in the Online Supplementary Information. Figure 3a plots bubble length as a function of P_d at various P_c values. The most important trend evident in the results is the severe dependence of L on pressure: with small (<10 %) change in P_d, the bubble length changes from the lowest values observed (roughly 200 μm) to over 600 μm before the onset of irregular coflow. The bubble generation frequency also shows a similarly strong dependence on pressure (Fig. 3b): the same few-percent changes in P_d induce a roughly twofold change in frequency. Incidentally, while it is not the focus of this paper, we mention in passing that the capillary number (calculated from the measured velocity and the surface tension between air and PDMS) ranges from 0.5 to 2.5 (Peng 2012).

Most drop microfluidic experiments in the literature are conducted in flow rate-controlled mode, and in those experiments, similar changes in drop size require much larger changes in relative flow rate of the two phases. For example, many researchers (Dietrich et al. 2008; Gordillo et al. 2004; Ganan-Calvo 2004; Ward et al. 2005) have found that drop length varies in a power-law fashion with the ratio of the flow rates of the two phases. Typically, the exponent is small—usually ranging from 0.25 to 0.4—thus indicating a weak dependence. The frequency dependence is also found to be weaker in flow rate-controlled experiments. To the best of our knowledge, the article by Ward et al. (2005) is the only publication to directly compare flow rate-controlled versus pressure-controlled drop generation in a single fluid system in a single microfluidic device. These authors conducted experiments on generating water drops with an oil matrix in a flow-focusing geometry and reported results that were very similar to those observed here: in pressure-controlled experiments, drops could be generated over a relatively narrow range of pressures, and the size of the drops varied strongly as pressure was changed. Similar to our experiments, they also reported that drops could not be generated if the pressure of the dispersed stream was too low because the dispersed phase could not penetrate into the contraction (Ward et al. 2005). They provided an empirical correlation that the drop length scaled as $\propto \left(\frac{P_d}{P_c}\right)^2$. However, this correlation must necessarily fail when the dispersed phase pressure reduces below the critical value at which drop generation stops, i.e., this empirical correlation must be restricted only to some finite range of pressures. More generally, it is not clear that the *ratio* of the two pressures, P_d/P_c, is the appropriate parameter to represent the results. This is because the absolute value of the pressure needed to drive the flow depends not only on the geometry of the drop-generating junction, but also on the channel lengths upstream or downstream of the junction. Thus, one may imagine two flow-focusing devices that are identical in all respects except that the downstream channel is very short in one device and very long in the other. If the pressures were adjusted to realize identical drop generation in both devices, the two devices would have very different P_d/P_c ratios; specifically, the device with the long downstream channel would have a P_d/P_c ratio approaching 1. One may be tempted to instead cast the results in terms of the pressure *difference* $(P_d - P_c)$ rather than the pressure *ratio*, but in this case, if for instance the dispersed phase channel supplying the junction was made much longer, identical drop generation would need a higher value of $(P_d - P_c)$.

Here, we will attempt modeling of pressure-controlled drop generation from the approach illustrated in Fig. 4a. We start by postulating that the local dynamics of bubble generation are essentially identical regardless of whether the flow is pressure-controlled or flow rate-controlled.

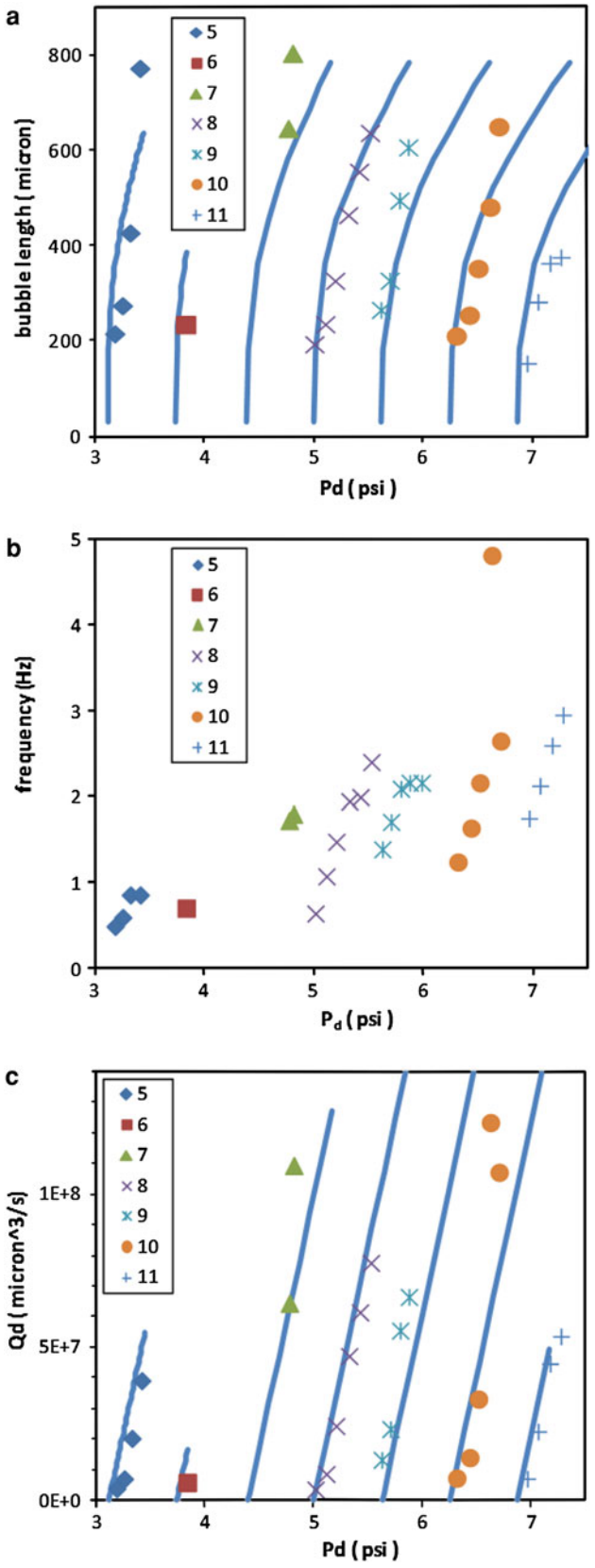

Fig. 3 **a** Bubble sizes, **b** bubble generation frequency, and **c** bubble flow rate measured experimentally. *Solid lines* in **a** and **c** are discussed in the text and correspond to Eqs. (12) and (7)

Thus, existing empirical or theoretical models of drop or bubble formation, which are usually expressed in terms of flow rates, should remain valid. The flow rates required in these models are unknown of course; our task then is to relate these unknown flow rates to the known pressures. In the following, we will derive a very simple "resistance circuit" model (Fig. 4b) of a pressure-controlled drop/bubble

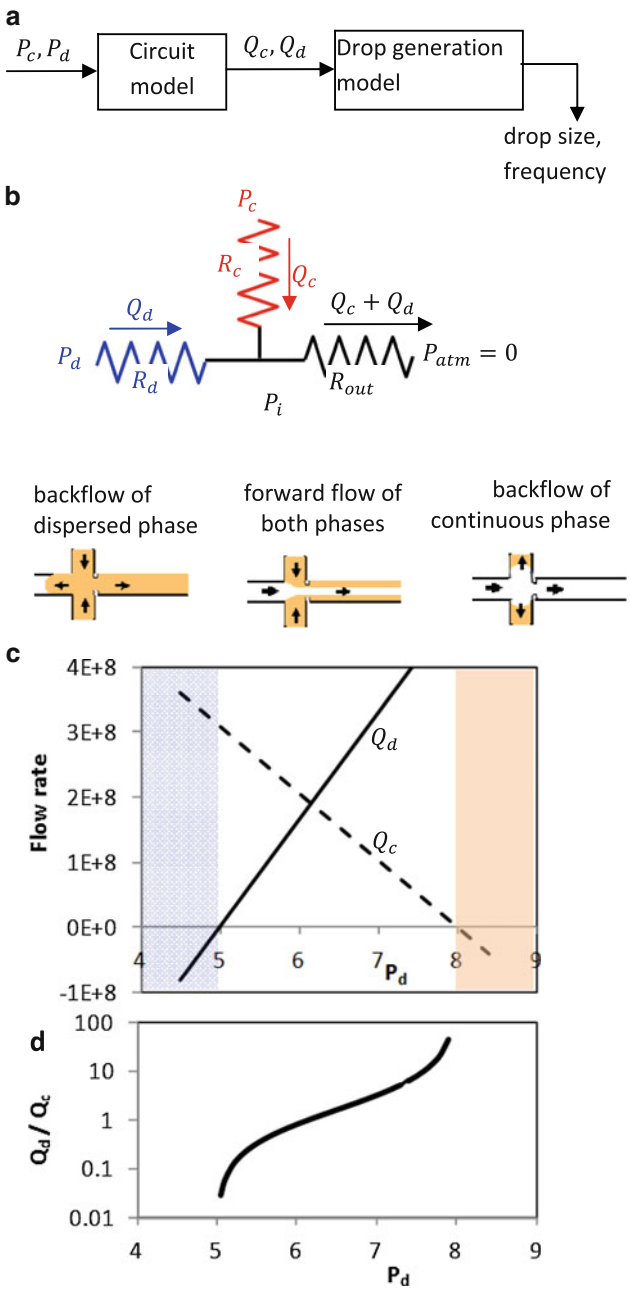

Fig. 4 **a** Modeling approach of calculating flow rates from pressures and drop sizes from flow rates. **b** Circuit diagram representing the microfluidic channels. Note that the resistance R_c represents both legs of the continuous fluid supply. **c** Flow rates as a function of pressure using the values $R_c = 9.7 \times$ psi.s/μm^3 and $R_c/R_{out} = 0.6$. **d** The ratio of flow rates Q_d/Q_c corresponding to **c**

generation device which relates flow rates to the pressures. Therefore, existing predictions for drop generation can be rewritten in terms of the applied pressures. We will show that the resulting equations very naturally capture the high pressure sensitivity of the drop generation.

3.1 Model

The essential idea of Fig. 4b is to relate the flow rates of each phase to the corresponding pressure drops via the flow resistances in each leg of the flow-focusing junction. One may therefore write

$$P_c - P_i = R_c Q_c \tag{1}$$

$$P_d - P_i = R_d Q_d \tag{2}$$

$$P_i - P_{\text{atm}} = R_{\text{out}}(Q_c + Q_d) \tag{3}$$

where P_i is the pressure at the intersection, and R_c, R_d, and R_{out} are the flow resistances of the continuous phase supply, dispersed phase supply, and the outlet channels, respectively. The outlet pressure P_{atm} will be arbitrarily set to zero. The flow resistances in the upstream legs of the channel, R_c and R_d, can be described by simple creeping flow equations and may be expected to be proportional to the channel length, proportional to the viscosity of the fluids flowing in those channels, and depend in some more complex fashion on the channel width and height. The resistance of the outlet leg is more complex since the flow in this channel is a two-phase flow. The flow resistance for a drop train varies in a complex way on the drop size and on the relative viscosity of the two phases (Ho and Leal 1975; Brenner 1971; Adzima and Velankar 2006; Olbricht 1996). Thus, Eq. (3) may be regarded as approximation to a more complex and likely nonlinear relationship between pressure drop and flow rate.

The above equations can be solved readily to obtain

$$P_i = \frac{-P_d R_c + P_c R_d}{R_d + R_c\left(\frac{R_d}{R_{\text{out}}} + 1\right)} \tag{4}$$

$$Q_d = \frac{-P_c + P_d\left(\frac{R_c}{R_{\text{out}}} + 1\right)}{R_d + R_c\left(\frac{R_d}{R_{\text{out}}} + 1\right)} \tag{5}$$

$$Q_c = \frac{-P_d + P_c\left(\frac{R_d}{R_{\text{out}}} + 1\right)}{R_d + R_c\left(\frac{R_d}{R_{\text{out}}} + 1\right)} \tag{6}$$

For our specific situation, since the dispersed phase is a gas, R_d is expected to be far less than R_c or R_{out}. Accordingly, Eqs. (5) and (6) can be rewritten as

$$Q_d = \frac{1}{R_c}\left[-P_c + P_d\left(\frac{R_c}{R_{\text{out}}} + 1\right)\right] \tag{7}$$

and

$$Q_c = \frac{1}{R_c}[-P_d + P_c] \tag{8}$$

Equation (7) suggests that the bubble flow rate varies linearly with both the pressures. In our experiment, the flow rates are not measured directly. However, the flow rate of the gas phase, Q_d, can be estimated by writing

$$Q_d = F \times V_{\text{bubble}} \tag{9}$$

The method of estimating bubble volume V_{bubble} from bubble images is described in the Online Supplementary Information. The corresponding plot of gas flow rate is shown as a function of P_d in Fig. 3c. An approximately linear dependence on P_d appears reasonable from the data, and indeed by adjusting the two parameters, R_c and R_c/R_{out} in Eq. (7), all of the data of Fig. 3c can be fitted simultaneously, suggesting that the model captures the basic physics of the problem. Later, we will compare the fitted values of $R_c = 9.7 \times \text{psi.s}/\mu\text{m}^3$ and $R_c/R_{\text{out}} = 0.6$ against estimates from creeping flow equations.

Having established that the circuit model is physically reasonable, we can now understand the reason why drop generation is highly sensitive to pressure. Figure 4c illustrates the behavior of the two flow rates as P_d is varied keeping P_c fixed at 8 ψ. This graph was drawn with the same values of R_c and R_c/R_{out} obtained above, and with $R_d = 0$; however, the comments below are general regardless of whether R_d is taken as zero or not. As P_d is increased at fixed P_c, the dispersed phase flow rate increases whereas the continuous flow rate decreases. Forward flow of both fluids requires that both Q_c and Q_d be positive:

$$Q_c > 0 \quad \text{hence} \frac{P_d}{P_c} < \frac{R_d}{R_{\text{out}}} + 1 \tag{10}$$

$$Q_d > 0 \quad \text{hence} \frac{P_d}{P_c} > \frac{R_{\text{out}}}{R_c + R_{\text{out}}} \tag{11}$$

Note that for our specific case, $\frac{R_c}{R_{\text{out}}} = 0.6$, and the corresponding Eq. (11) plotted as a solid line in Fig. 2g captures the onset of bubble formation well. Furthermore, R_d is small and hence Eq. (10) simplifies to $P_d < P_c$. This is shown as a dashed line in Fig. 2g and lies far above the data; our experiments were stopped at the onset of coflow and such high values of P_d were not examined.

These equations identify the range of pressures within which two-phase flow may be expected; outside of this range, backflow will occur and the dispersed phase will invade the inlet of the continuous phase or vice versa. The noteworthy feature is that near the ends of this pressure range, the ratio of the flow rates Q_d/Q_c is highly sensitive to pressure changes as illustrated in Fig. 4d. This provides a simple explanation for the high sensitivity of the drop

generation process to pressure. Specifically, many articles have shown that the drop length scales as

$$L = \beta\left(\frac{Q_d}{Q_c}\right)^{\alpha} = \beta\left(\frac{-P_c + P_d\left(\frac{R_c}{R_{\text{out}}} + 1\right)}{-P_d + P_c}\right)^{\alpha} \tag{12}$$

where the latter equality is obtained from substituting Eqs. (7) and (8). Values of α values ranging from 0.25 to 0.4 have been reported. Regardless of the exact value, since the ratio Q_d/Q_c is predicted to be highly sensitive to pressure, so too must be the bubble lengths. In particular, Eq. (12) suggests that the drop length will reduce sharply as the minimum P_d [corresponding to Eq. (11)] is approached. Indeed, a value of $\alpha = 1/3$ provides good fits to the measured data (solid lines in Fig. 3c) with the prefactor β (which captures the geometry and viscosity dependence) as the sole fitting parameter. We emphasize that in obtaining the solid lines in Fig. 3c, the ratio of the resistances was not varied; R_c/R_{out} was kept fixed at 0.6 as found from Fig. 3a. It is important to recognize that—as compared to the empirical correlation $L \propto \left(\frac{P_d}{P_c}\right)^2$ presented by Ward et al.(Ward et al. 2005)—Eq. (12) is automatically limited to a finite pressure range within which two-phase flow is possible. Incidentally, referring back to the comments at the end of the Sect. 3, Eq. (12) also shows that the drop length is neither a simple function of the pressure *ratio* nor of the pressure *difference*; thus, representing the drop formation in terms of either of those quantities would not be appropriate.

We may also compare the values of the resistances obtained from the fits to those expected from creeping flow equations. One direct comparison may be made by evaluating the *total* resistance of the microfluidic channels from the inlet (pressure P_c) to the outlet at atmospheric pressure. The calculations are illustrated in the Online Supplementary Information. The net resistance calculated, 4.6×10^{-8} psi.s/m^3, is on the same order of magnitude as $(R_c + R_{\text{out}}) = 2.6 \times 10^{-8}$psi.s/$\mu$m^3 obtained from the fitting. A second comparison may be made of the value of R_c/R_{out}. This is potentially more complicated since it requires a judgment of what portion how the junction resistance (R_3 in the notation of Fig. S1) is to be split between the upstream and downstream channels. However, in our specific case, the value of the junction resistance is small and makes little difference how it is split. If we arbitrarily assign half of the junction resistance to the upstream and the other half to the downstream channel, $R_c/R_{\text{out}} = 0.38$ is found as compared with 0.6 from the fitting. In both comparisons, the discrepancies are significant, but perhaps not unreasonable given the assumptions that the two-phase downstream channel can be treated as a single-phase flow of the continuous phase, and that interfacial phenomena associated with drop formation do not contribute to the pressure.

We have also conducted limited experiments (Peng 2012) with PDMS of viscosities 10 and 500 Pa.s. We find that the minimum gas pressure required to initiate bubbles does not change with viscosity and that the Q_d versus P_d data can be fitted with nearly the same value of R_c/R_{out}, with R_c being roughly proportional to viscosity. All of these observations are consistent with the circuit model.

To summarize, these results indicate that the basic idea of Fig. 4a—relate the pressures to the flow rate, and the flow rates to the drop formation—appears reasonable. The high sensitivity of the drop formation process to pressure is chiefly because the ratio of the flow rates is sensitive to pressure. Indeed, if R_c/R_{out} is small, the pressure range specified by Eqs. (10) and (11) becomes small, i.e., two-phase flow, and hence, bubble generation can happen over only a very narrow range of pressures and the process becomes especially sensitive to pressure. This immediately suggests a way to reduce the sensitivity, viz. to keep the value of R_c/R_{out} large. Practically, this may be done by minimizing the flow path length downstream of the junction and/or increasing the channel cross sectional dimensions downstream of the junction. It must be emphasized that the circuit model does not account for any details of drop formation; it only seeks to identify whether two-phase flow will occur or not. Thus, Eq. (12) predicts L can approach very small or very large values, whereas in our experiments [or in the experiments of Ward et al. (Ward et al. 2005)], drops much smaller than channel dimensions were never observed. More sophisticated models of drop formation may be used instead of Eq. (12), which may predict that upon onset of bubble formation, the bubbles already have a certain minimum size rather than $L = 0$.

Finally, we will comment briefly on generating drops rather than bubbles in this microfluidic device. As mentioned in the Introduction, the motivation underlying this project is to develop two-phase molten polymer microfluidics to prepare particles from thermoplastic polymers. Accordingly, we have also conducted experiments using a polymer, polyisoprene, as the dispersed phase. Like PDMS, this polymer is liquid at room temperature, and hence, we were able to test the possibility of drop formation at room temperature. In the device described above, drop formation was generally not observed; instead, a coflow was observed in which a filament of PI flowed through the center of the channel, surrounded by the PDMS continuous phase. This filament was highly stable all the way from the junction to the exit of the device. Such filament formation was dubbed "threading" previously (Cubaud and Mason 2008). Limited experiments with fluids of viscosity intermediate between air and polyisoprene suggest that the filament formation is attributable to viscosity ratio effects (Peng 2012).

We have also conducted additional experiments with a different microfluidic device with substantially smaller dimensions, and in this case, filaments were observed to breakup far downstream in the channel into a sequence of drops. These results, some of which are shown in the Online Supplementary Information, suggest that in spite of the high viscosity of polymers, microfluidic generation of drops by passive drop breakup is indeed possible. We are conducting research on operating this device at a high temperature with thermoplastic polymers so that the drops may then be frozen into particles.

4 Conclusion and future prospects

In summary, we have examined bubble generation in a pressure-controlled microfluidic device. This article makes two chief contributions. First, our results suggest that the high sensitivity of bubble size to pressure may simply be a consequence of the fact that in a pressure-controlled flow, two-phase flow is possible only in a finite pressure window. Near the ends of this window, the relative flow rate of the two fluids is highly sensitive to pressure, and hence so is bubble generation. A simple circuit model which relates pressures to flow rates is able to capture the main features of bubble generation. The circuit model also suggests that minimizing the flow resistance downstream of the drop-generating junction will reduce the sensitivity and expand the window of pressures within which bubbles may be generated.

Second, we have extended previous research (Moon and Migler 2010; Moon et al. 2008) on polymer melt microfluidics toward drop generation devices. We show that in spite of the high viscosity of polymers, drop generation is indeed possible, and in fact, because drops are generated by a downstream capillary instability, the drop size can be much smaller than the device dimensions. Moreover, creating multilayer devices is no more difficult than creating single layer devices, thus allowing complex flow paths to be realized (Moon and Migler 2010). While this research was conducted at room temperature, the metal foil-based fluid channels and the fluid-handling approach are both well-suited for handling thermoplastic polymers. In particular, since the channels are etched in metal foil, they can withstand temperatures of 300 °C, adequate for almost all thermoplastic polymers. Such metal foil-based devices are not limited to polymers either. Recently microfluidic drop generation of room temperature-liquid metal has been demonstrated (Thelen et al. 2012); using a high temperature device based on metal foils, the same research could be extended to metals that are solid at room temperature. The chief challenge of conducting research at high temperatures is window materials: while sapphire or glass can easily handle temperatures of 300 °C, constructing devices with windows that are thin enough to accommodate the small working distance of microscope objectives is challenging. Finally, we note that such particle fabrication using thermoplastic polymers is readily scalable. The polymer industry routinely manufactures multicomponent polymer fibers from a variety of plastics by extrusion (Fourné 1998; Nakajima 2000). The corresponding extruder feed blocks, made by traditional machining or chemical etching techniques, combine multiple molten polymers streams along extremely complex pathways to extrude as many as 100 fibers simultaneously (Hills 1992). Thus, if the technology of controlling interfacial tension-driven filament breakup is developed, it can be scaled up readily using existing plastic extrusion techniques.

Acknowledgments This research was partly funded by NSF-CBET Grants #0932901 and CBET-0448845. We are grateful to Drs. Steven Hudson, Kalman Migler, and Doyoung Moon from NIST for valuable advice on device design and for Mr. Alex Boardman for assisting with the experiments.

References

Adzima BJ, Velankar SS (2006) Pressure drops for droplet flows in microfluidic channels. J Micromech Microeng 16(8):1504–1510

Anna SL, Bontoux N, Stone HA (2003) Formation of dispersions using "flow focusing" in microchannels. Appl Phys Lett 82(3): 364–366

Bong KW, Chapin SC, Pregibon DC, Baah D, Floyd-Smith TM, Doyle PS (2010) Compressed-air flow control system. Lab Chip 11(4):743–747. doi:10.1039/c0lc00303d

Brenner H (1971) Pressure drop due to the motion of neutrally buoyant particles in duct flows II. Spherical drops and bubbles. Ind Eng Chem Fundam 4:537

Chen C-H, Shah RK, Abate AR, Weitz DA (2009) Janus particles templated from double emulsion droplets generated using mcro-fluidics. Langmuir 25(8):4320–4323. doi:10.1021/la900240y

Christopher GF, Anna SL (2007) Microfluidic methods for generating continuous droplet streams. J Phys D Appl Phys 40(19):R319–R336. doi:10.1088/0022-3727/40/19/r01

Cubaud T, Mason TG (2008) Capillary threads and viscous droplets in square microchannels. Phys Fluids 20(5). doi:053302 10.1063/1.2911716

Cubaud T, Tatineni M, Zhong XL, Ho CM (2005) Bubble dispenser in microfluidic devices. Phys Rev E 72 (3). doi:037302 10.1103/PhysRevE.72.037302

Dendukuri D, Tsoi K, Hatton TA, Doyle PS (2005) Controlled synthesis of nonspherical micro particles using microfluidics. Langmuir 21(6):2113–2116. doi:10.1021/la047368k

Dietrich N, Poncin S, Midoux N, Li HZ (2008) Bubble formation dynamics in various flow-focusing microdevices. Langmuir 24(24):13904–13911. doi:10.1021/la802008k

Fourné F (ed) (1998) Synthetic fibers. Hanser Verlag, Munich

Ganan-Calvo AM (2004) Perfectly monodisperse microbubbling by capillary flow focusing: An alternate physical description and universal scaling. Phys Rev E 69(2):027301. doi:10.1103/PhysRevE.69.027301

Garstecki P, Gitlin I, DiLuzio W, Whitesides GM, Kumacheva E, Stone HA (2004) Formation of monodisperse bubbles in a microfluidic flow-focusing device. Appl Phys Lett 85(13): 2649–2651

Gordillo JM, Cheng ZD, Ganan-Calvo AM, Marquez M, Weitz DA (2004) A new device for the generation of microbubbles. Phys Fluids 16(8):2828–2834

Hills WH (1992) Method of making plural component fibers. USA Patent 5162074

Ho BP, Leal LG (1975) Creeping motion of liquid drops through a circular tube of comparable diameter. J Fluid Mech 71:361–384

Kumacheva E, Garstecki P (2011) Microfluidic reactors for polymer particles. Wiley, Chichester

Marre S, Jensen KF (2010) Synthesis of micro and nanostructures in microfluidic systems. Chem Soc Rev 39(3):1183–1202. doi: 10.1039/b821324k

Moon D, Migler KB (2010) Forced assembly and mixing of melts via planar polymer micro-mixing. Polymer 51(14):3147–3155. doi: 10.1016/j.polymer.2010.04.070

Moon D, Bur AJ, Migler KB (2008) Multi-sample micro-slit rheometry. J Rheol 52(5):1131–1142. doi:10.1122/1.2955511

Nakajima T (2000) Advanced fiber spinning technology. Woodhead Publishing, Cambridge

Nie ZH, Li W, Seo M, Xu SQ, Kumacheva E (2006) Janus and ternary particles generated by microfluidic synthesis: design, synthesis, and self-assembly. JACS 128(29):9408–9412. doi: 10.1021/ja060882n

Olbricht WL (1996) Pore-scale prototypes of multiphase flow in porous media. Ann Rev Fluid Mech 28:187–213

Peng S-C (2012) Microfludic drop formation with polymer melts. M.S. thesis, University of Pittsburgh, Pittsburgh

Serra CA, Chang Z (2008) Microfluidic-assisted synthesis of polymer particles. Chem Eng Technol 31(8):1099–1115. doi:10.1002/ceat.200800219

Shum HC, Abate AR, Lee D, Studart AR, Wang B, Chen C-H, Thiele J, Shah RK, Krummel A, Weitz DA (2010) Droplet microfluidics for fabrication of non-spherical particles. Macromol Rapid Comm 31(2):108–118. doi:10.1002/marc.200900590

Stone HA, Stroock AD, Ajdari A (2004) Engineering flows in small devices: microfluidics toward a lab-on-a-chip. Ann Rev Fluid Mech 36:381–411

Sugiura S, Nakajima M, Iwamoto S, Seki M (2001) Interfacial tension driven monodispersed droplet formation from microfabricated channel array. Langmuir 17(18):5562–5566

Thelen J, Dickey MD, Ward T (2012) A study of the production and reversible stability of EGaIn liquid metal microspheres using flow focusing. Lab Chip 12(20):3961–3967

Thorsen T, Roberts RW, Arnold FH, Quake SR (2001) Dynamic pattern formation in a vesicle-generating microfluidic device. Phys Rev Lett 86(18):4163–4166

Ward T, Faivre M, Abkarian M, Stone HA (2005) Microfluidic flow focusing: drop size and scaling in pressure versus flow-rate-driven pumping. Electrophoresis 26(19):3716–3724